

*This paper reports a study into the role of individual (S, P, N, C, Si, Mn, Ni, Cr) and combined ( $Q_1=S$ ,  $Q_2=S+P$ ,  $Q_3=S+P+N$ ,  $Q_4=S+P+N+C$ ,  $Q_5=S+P+N+C+Si$ ,  $Q_6=S+P+N+C+Si+Mn$ ,  $Q_7=S+P+N+C+Si+Mn+Ni$ ,  $Q_8=S+P+N+C+Si+Mn+Ni+Cr$ ) elements in five steel AISI 304 smelting cycles. The correlation between the rate of corrosion  $K$  in chloride-containing media and the specific magnetic susceptibility  $\chi_0$  of austenite (matrix), the low content  $P_\delta$  of  $\delta$ -ferrite, and the percentage of elements has been established. Taking into consideration the order of arrangement and influence of other present components, a set of the different-shaped graphic models of  $K$  dependences on  $\chi_0$ ,  $P_\delta$ , and percentage of elements was found. However, the sum of the eight calculated individual and combined elements ( $Q_8$ ) of the models coincides with the sum of the same elements ( $Q=Q_8$ ) of steel smelting samples that were subjected to experimental measurements of  $\chi_0$  and  $P_\delta$ . The curves of the reported models were compared with experimental dependences of  $K$  on  $\chi_0$ ,  $P_\delta$ . The positive and negative role of individual and combined elements in the process of pitting resistance of steel smelting cycles has been identified. Given this, it is assumed that the effect exerted on  $K$  by individual and combined elements in the intervals before and after their critical content may be ambiguous. Hence, one value  $K$  can correspond to several values of the contents of elements,  $\chi_0$ ,  $P_\delta$ . A proof of that is the coincidence between the calculated models  $K$  of corrosion on the same total content of  $Q_8$  for steel samples determined experimentally. The positive (negative) and ambiguous role of elements in the process of corrosion and the possibility of predicting corrosion tolerance of austenitic steels are assumed. The experimental dependence  $K$  on  $\chi_0$  and  $P_\delta$  has been established; the greater  $c_0$  and  $P_\delta$ , the lower the corrosion rate  $K$ . The studied steels contained  $\delta$ -ferrite in the low limits of 0.01...0.1 %*

**Keywords:** steel AISI 304, corrosion, magnetic susceptibility, ferrite, magnetic moment, nickel, chromium, chloride-containing medium

# DETERMINING THE ROLE OF INDIVIDUAL AND COMBINED CHEMICAL ELEMENTS IN THE PITTING CORROSION PROCESS OF AUSTENITIC Fe-Cr-Ni STEELS

**Valentin Snizhnoi**

PhD, Associate Professor

Department of General and Applied Physics

Zaporizhzhia National University

Zhukovskoho str., 66, Zaporizhzhia, Ukraine, 69600

**Gennadii Snizhnoi**

Corresponding Author

Doctor of Technical Sciences, Associate Professor,

Head of Department\*

E-mail: snow@zp.edu.ua

**Sergiy Stepanenko**

PhD, Associate Professor\*

\*Department of Micro- and Nanoelectronics

Zaporizhzhia Polytechnic National University

Zhukovskoho str., 64, Zaporizhzhia, Ukraine, 69063

Received date 24.04.2022

**How to Cite:** Snizhnoi, V., Snizhnoi, G., Stepanenko, S. (2022). Determining the role of individual and combined chemical elements in

Accepted date 21.06.2022

the pitting corrosion process of austenitic Fe-Cr-Ni steels. Eastern-European Journal of Enterprise Technologies, 3 (12 (117)), 13–19.

Published date 30.06.2022

doi: <https://doi.org/10.15587/1729-4061.2022.257841>

## 1. Introduction

The widespread use of austenitic chromium-nickel steels in the chemical and pharmaceutical industry, mechanical engineering, and energy generation requires further study of corrosion resistance. To investigate pitting corrosion, various methods are used, with the help of which significant progress has been achieved [1]. The concentration of alloyed elements in different steel grades corresponds to the expected corrosion resistance. Difficulties arise in finding out the causes of unequal corrosion resistance for different smelting cycles of the same steel grade, in which the content of chemical elements is very close. This necessitates finding new directions for the study of corrosion in order to improve the performance of articles. Hence, the introduction of a new magnetometric method is relevant, which is based on the establishment of a correlation relationship between the corrosion rate and the specific magnetic susceptibility of austenite (matrix), low  $\delta$ -ferrite content, and the percentage of elements using the steel AISI 304 as an example.

Considerable attention is paid to the study of local corrosion of the steel AISI 304 in order to obtain direct practical results. Paper [2] reports improvements in corrosion resistance after plasma nitriding. A high intensity of corrosion is observed in the grids of the separator, which are subject to the influence of humidity of air contaminated with hydrogen sulfide [3]. The influence of low-energy grain boundaries in steels on increasing the plasticity of articles is considered in [4]. Grinding grains improves corrosion tolerance of steel [5].

In [6], it is proved that the pitting resistance of the steel AISI 304 decreases with an increase in boron content. In [7], it is shown that the corrosion rate of the steel AISI 304 varies due to the concentration of Cl ions. In the steel AISI 304 corrosion is observed with the participation of copper ions and mechanical stresses [8]. Study [9] confirmed the combined synergistic effect of Mo and N, rather than the addition of their individual elements [9].

Hence, despite numerous studies into corrosion processes, emerging problems require new approaches to the

study of the role of both individual and combined elements on the pitting corrosion of austenitic chromium-nickel steels.

## 2. Literature review and problem statement

The pitting corrosion of austenitic chromium-nickel steels was investigated by classical methods (chemical, electrochemical, etc.) in a large number of scientific works. Magnetometry is much less used. Thus, work [10] established a correlation between the type of a corrosion defect and the magnitude of the magnetic susceptibility of the steel 12X18N10T sample from those zones in which defects are localized. It is shown that corrosion in the studied fragment of the sample is due to the depletion of a solid solution of austenite chromium. In these places, carbides and  $\alpha$  phase also occur. This makes it possible to identify by magnetic methods potentially dangerous areas in steel even before the occurrence of corrosion defects.

In work [11], it was found that in the steels AISI 304 and AISI 321 with an increase in the specific magnetic susceptibility of austenite and low content of  $\delta$ -ferrite, the rate of pitting corrosion decreases. The ambiguous role of carbon and nitrogen on the corrosion rate has been identified, that is, several values of the carbon or nitrogen content can correspond to one value of corrosion speed.

The theory of the origin of re-passivation and growth of metastable and stable pits on the surface of corrosion-tolerant steels is presented in work [12]. The mechanisms and patterns of corrosion dissolution of Cr, Ni, and Fe in the steel AISI 304 were established in [13]. Cr and Ni have been shown to contribute to the decline, and Mn to increase the selective dissolution coefficient of Cr [14]. It is proved that in the steel AISI 304 after the first and second cycles of testing, corrosion losses increase with an increase in the content of Cu, Si, and a decrease in Ni [15]. It is established that the loss of iron  $\Delta Fe$  in the steel AISI 321 from stable pits decreases with an increase in pits in it of Cr content [16]. The selective nature of dissolution of the main components Cr, Ni, Fe from pits on the surface of the steels 08X18H10, AISI 321, AISI 316 [17] is shown. Electrochemical corrosion of the steel AISI 304 decreased with an increase in deformation to 20 % and increased with deformation of 35 % [18]. Removal of tendencies to pitting corrosion by the austenitic Cr-Ni steels is achieved through the combined doping of N and Mo [19]. Elements Mo and W improve passivity and resistance to destruction in the initial stages of local corrosion of chromium-nickel steels [20]. The formation of  $\delta$ -ferrite does not impair or prevent corrosion tolerance of the steel AISI 304 [21]. Doping the alloy FeCrMnMoNC with Mo increases the tolerance of pitting corrosion [22]. The improvement of corrosion resistance by alloying with Si and Mn of austenite stainless steels has been confirmed in [23]. The formation of a passive layer enriched with Cr, Ni, Mn, and Fe causes inhibition of corrosion processes of the steel AISI 304 [24].

Our review of literary data [10–24] reveals that there are unresolved issues that are associated with the influence of each element in the smelting cycles of one steel grade on the rate of pitting corrosion in the presence of all other components of austenitic chromium-nickel steels. Additionally, the role of combined elements consistently added to each other has not been studied for corrosion. Experimentally

solving these issues is difficult. The option of overcoming the relevant difficulties may be our proposed magnetometric approach.

## 3. The aim and objectives of the study

The aim of this study is to determine the role of individual and combined chemical elements (in the presence of others) on the process of local pitting corrosion in the steel AISI 304. This will make it possible to identify the cause of change in corrosion rate in the smelting cycles of one steel grade.

To achieve the set aim, the following tasks have been solved:

- to establish the effect of individual elements S, P, N, C, Si, Mn, Ni, Cr in the presence of others on the local pitting corrosion of five steel AISI 304 smelting cycles with the help of specific magnetic susceptibility of austenite and low content of  $\delta$ -ferrite;

- to establish the influence of sequentially added elements (one of a set of models of coexistence of elements):  $Q_1=S$ ,  $Q_2=S+P$ ,  $Q_3=S+P+N$ ,  $Q_4=S+P+N+C$ ,  $Q_5=S+P+N+C+Si$ ,  $Q_6=S+P+N+C+Si+Mn$ ,  $Q_7=S+P+N+C+Si+Mn+Ni$ ,  $Q_8=S+P+N+C+Si+Mn+Ni+Cr$  (% by weight) on the corrosion process using specific magnetic susceptibility of austenite and low  $\delta$ -ferrite content.

## 4. The study materials and methods

Five smelting cycles of the industrial sheet steel AISI 304 with a thickness of 1 mm were investigated; their chemical composition is given in Table 1.

Table 1

Chemical composition of the steel AISI 304 (% by weight)

Smelting cycle No.	S	P	N	C	Si	Mn	Ni	Cr
1	0.001	0.027	0.048	0.071	0.22	1.23	9.34	17.96
2	0.001	0.028	0.046	0.067	0.50	1.74	8.09	18.22
3	0.004	0.024	0.055	0.075	0.43	1.65	8.09	18.25
4	0.002	0.028	0.044	0.050	0.41	1.70	8.10	18.30
5	0.001	0.034	0.039	0.030	0.39	1.81	8.20	18.10

Since the low content of  $\delta$ -ferrite across the width of the sheet is distributed locally unevenly, so in a chess order from different places of each smelting cycle, we cut 7...10 samples in the shape of parallelepipeds measuring  $\sim 7 \times 3 \times 1$  mm<sup>3</sup>. Surfaces were polished with subsequent electric polishing. Then we determined at a magnetometric installation of the type of Faraday scales in magnetic fields  $H=(3.0...5.0) \times 10^5$  A/m the average values of specific susceptibility of austenite  $\chi_0$  and low content of  $\delta$ -ferrite  $P_\delta$  according to the procedure from [25]. The corrosion rate  $K$  in the chlorine-containing environment (GOST 9.91289) of the steel AISI 304 (Thyssen Krupp, 1.45 41, Germany) is borrowed from [26].

The total content of all elements added to each other sequentially in order of mass gain  $Q_1...Q_8$  and the final sum  $Q$  of each steel AISI 304 smelting cycle are given in Table 2 (one of the sets of models).

Table 2

The total content of all chemical elements added to each other sequentially by ordinal increase in mass  $Q_1...Q_8$

Smelting cycle No.	% by weight							
	$Q_1$	$Q_2$	$Q_3$	$Q_4$	$Q_5$	$Q_6$	$Q_7$	$Q_8$
1	0.001	0.028	0.076	0.147	0.367	1.597	10.937	28.897
2	0.001	0.029	0.075	0.142	0.642	2.382	10.472	28.692
3	0.004	0.028	0.083	0.158	0.588	2.238	10.328	28.578
4	0.002	0.030	0.074	0.124	0.534	2.234	10.334	28.634
5	0.001	0.035	0.074	0.104	0.434	2.304	10.504	28.604

5. Results of studying the role of the content of individual and combined chemical elements on  $K$ ,  $\chi_0$  of austenite,  $P_\delta$

5.1. Effect of the content of individual chemical elements on  $K$ ,  $\chi_0$ ,  $P_\delta$

The values of corrosion speed  $K$ , specific magnetic susceptibility of austenite  $\chi_0$ , low content of  $\delta$ -ferrite  $P_\delta$ , and the total mass composition of chemical elements  $Q_8$  for each steel AISI 304 smelting cycle are given in Table 3.

Table 3

Values of  $K$ ,  $\chi_0$  of austenite,  $P_\delta$   $\delta$ -ferrite,  $Q_8$  for each AISI 304 steel smelting cycle

Smelting cycle No.	$K$ , g/(m <sup>2</sup> h)	$\chi_0$ , 10 <sup>-8</sup> m <sup>3</sup> /kg	$P_\delta$ , %	$Q_8$ , % by weight
1	47.65	2.27	0.0335	28.897
2	57.76	2.25	0.0448	28.692
3	86.64	2.23	0.0138	28.578
4	43.37	2.31	0.1130	28.634
5	67.87	2.24	0.0329	28.604

The analysis of Tables 1, 3 reveals that the chemical composition of all five smelting cycles meets the AISI 304 steel standard but the values of corrosion rate  $K$ , specific magnetic susceptibility  $\chi_0$  of austenite, and low  $\delta$ -ferrite content  $P_\delta$  vary significantly.

Fig. 1–7 illustrate a correlation between the rate of pitting corrosion  $K$ , the specific magnetic susceptibility  $\chi_0$  of austenite, low  $\delta$ -ferrite content  $P_\delta$  and the percentage content on the example of individual chemical elements P, C, Mn, Cr in the steel AISI 304. Numbers near the points are the numbers of smelting cycles. The parabolic curves of dependences  $K$ ,  $\chi_0$  and  $P_\delta$  on the concentration of elements (Fig. 1–3, 5–7) contain points (min or max) of critical contents of individual elements, before and after which the rate of pitting corrosion decreases or increases.

Fig. 1 shows the correlation between the corrosion rate  $K$  and the content of individual chemical elements of phosphorus and carbon.

The mirror nature of the effect of elements P and C on the corrosion rate  $K$  in intervals before and after their critical contents is observed. Namely, the corrosion rate  $K$  for P in the intervals up to the critical content ( $P_c=0.028\%$  by weight) increases, and then decreases. For C, the situation is mirrored ( $C_c=0.050\%$  by weight). This means that, taking into consideration the numbers of smelting cycles, the trend of change will be the opposite. For P, we have smelting 3→smelting 2→smelting 1→smelting 4( $P_c$ )→smelting 5. And for element C, the direction of change is as follows: smelting 5→smelting 4( $C_c$ )→smelting 1→smelting 2→smelt-

ing 3. The ambiguous result of Si's effect on corrosion tolerance of the steel X16N15M3 and X18H11 is given in [19].

Fig. 2 shows the correlation between the specific magnetic susceptibility  $\chi_0$  of austenite and the content of individual elements P and C.

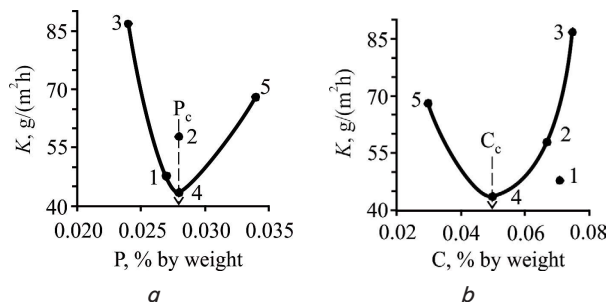


Fig. 1. Correlation between the corrosion rate  $K$  and the content of individual chemical elements: a – phosphorus; b – carbon

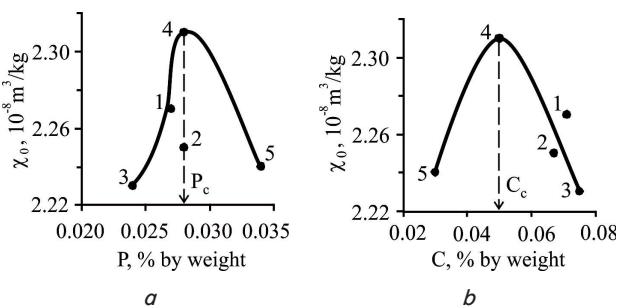


Fig. 2. Correlation between austenite's  $\chi_0$  and the content of individual chemical elements: a – phosphorus; b – carbon

Similar to the rate of corrosion  $K$ , shown in Fig. 1, the mirror nature of the influence of P and C on  $\chi_0$  is manifested.

The experimental dependence of  $K$  on  $\chi_0$  and  $P_\delta$  of the steel AISI 304 samples is shown in Fig. 3. We have that the greater  $\chi_0$  and  $P_\delta$ , the lower the corrosion rate  $K$  [27]. Comparing the estimated curves in Fig. 2 with experimental curves in Fig. 3, we have a proof of obtaining a correlation between the corrosion rate  $K$  and the content of individual elements P and C (Fig. 1). This proof, for example, for P, is explained as follows: the value of  $\chi_0$  increases with an increased content of  $P_\delta$  according to the scheme: smelting 3→smelting 2→smelting 1→smelting 4 (Fig. 2, a), and, in the direction of smelting 4→smelting 5,  $\chi_0$  decreases.

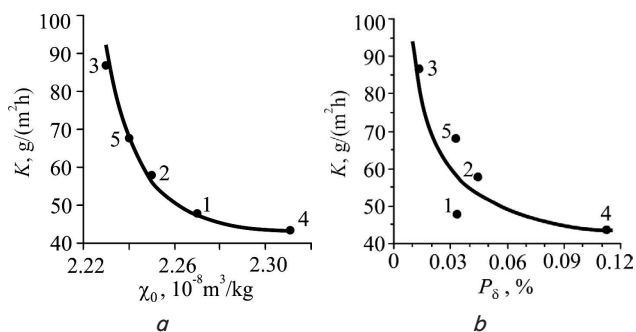


Fig. 3. Experimental dependence of the corrosion rate  $K$  of the steel AISI 304 on: a – specific magnetic susceptibility  $\chi_0$  of austenite; b –  $\delta$ -ferrite content  $P_\delta$

Fig. 4 illustrates the correlation between  $\delta$ -ferrite  $P_\delta$  and the content of individual elements P and C.

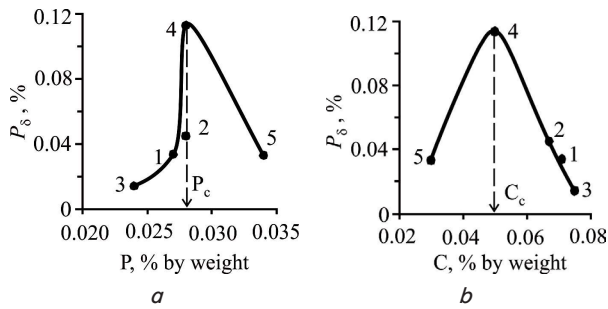


Fig. 4. Correlation between  $\delta$ -ferrite  $P_\delta$  and the content of individual chemical elements: *a* – phosphorus; *b* – carbon

Similar to the rate of corrosion  $K$ , shown in Fig. 1, the mirror nature of the influence of P and C on  $P_\delta$  is observed. Comparing the estimated curves in Fig. 4 with experimental curves in Fig. 3, we have a proof of obtaining a correlation between the corrosion rate  $K$  and the content of individual elements P and C.

The correlation between  $K$  and the content of individual elements Mn and Cr is illustrated in Fig. 5.

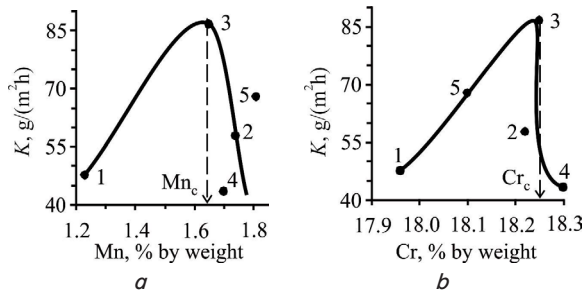


Fig. 5. Correlation between austenite's  $\chi_0$  and the content of individual chemical elements: *a* – manganese; *b* – chromium

The components Mn and Cr affect  $K$  in the same direction (except smelting cycle 5) in intervals before and after critical contents and play both a positive and negative role.

Fig. 6 shows the correlation between  $\chi_0$  and the content of individual elements Mn and Cr.

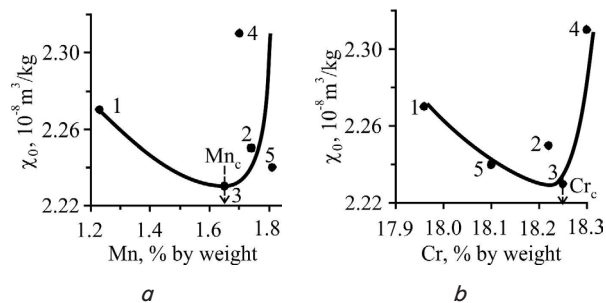


Fig. 6. Correlation between austenite's  $\chi_0$  and the content of individual chemical elements: *a* – manganese; *b* – chromium

Comparing the estimated curves in Fig. 6 with experimental curves in Fig. 3, we have a proof of the correlation between the corrosion rate  $K$  and the content of individual elements Mn and Cr.

The correlation between  $P_\delta$  and the content of individual elements Mn and Cr is shown in Fig. 7.

Comparing the estimated curves in Fig. 7 with experimental curves in Fig. 3, we have a proof of the correlation between the corrosion rate  $K$  and the content of individual elements Mn and Cr.

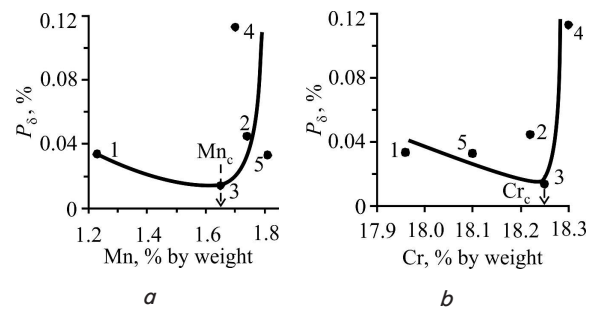


Fig. 7. Correlation between  $\delta$ -ferrite  $P_\delta$  and the content of individual chemical elements of manganese: *a* – manganese; *b* – chromium

### 5.2. The role of the content of combined chemical elements on $K$ , $\chi_0$ , $P_\delta$

Fig. 8–13 demonstrate the results of the correlation between the rate of pitting corrosion  $K$ , specific magnetic susceptibility  $\chi_0$  of austenite, low  $\delta$ -ferrite content  $P_\delta$  and percentage content on the example of combined elements  $Q_2=S+P$ ,  $Q_4=S+P+N+C$ ,  $Q_6=S+P+N+C+C+Si+Mn$ ,  $Q_8=S+P+N+C+Si+Mn+Ni+Cr$  of the steel AISI 304. Numbers near the points are the numbers of smelting cycles.

It should be noted that Fig. 8–13 depict one of the sets of models of the sample series of arrangements of combined elements ( $Q_1=S$ ,  $Q_2=S+P$ ,  $Q_3=S+P+N$ ,  $Q_4=S+P+N+C$ ,  $Q_5=S+P+N+C+Si$ ,  $Q_6=S+P+N+C+Si+Si+Mn$ ,  $Q_7=S+P+N+C+Si+M+Ni$ ,  $Q_8=S+P+N+C+Si+Si+Ni+Cr$ ). The shape of the curves in each model is different. This is because in addition to the combined elements, other elements with different contents act on corrosion.

However, regardless of the order of location of the elements, the sum of their percentage contents  $Q_8$  in each model remains unchanged, that is, equal to the sum  $Q$  of all alloying elements contained in the samples from all smelting cycles ( $Q=Q_8$ ). In this case, this is based on the fact that  $\chi_0$  and  $P_\delta$  have been experimentally determined for these samples.

Fig. 8 shows the correlation between the rate of pitting corrosion  $K$  and the total content of the combined elements  $Q_2=S+P$  (Fig. 8, *a*) and  $Q_4=S+P+N+C$  (Fig. 8, *b*)

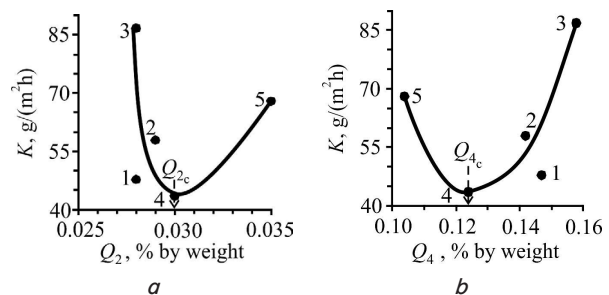


Fig. 8. Correlation between the rate of pitting corrosion  $K$  and the total content of combined chemical elements: *a* –  $Q_2$ ; *b* –  $Q_4$

There is a mirror nature of the effect of elements  $Q_2=S+P$  and  $Q_4=S+P+N+C$  on the corrosion rate  $K$  in the intervals before and after their critical contents. Namely,  $K$  for  $Q_2$  falls to a critical content (smelting 4) (smelting 3→smelting 2→smelting 1→smelting 4), and then increases (smelting 4→smelting 1).

Fig. 9 shows the correlation between  $\chi_0$  and the total content of the combined elements  $Q_2$  and  $Q_3$ .

Similar to  $K$  (Fig. 8), the mirror nature of the effects of  $Q_2$  and  $Q_4$  on austenite's  $\chi_0$  is manifested.

Fig. 10 illustrates the correlation between  $P_\delta$  and the total content of the combined elements  $Q_2$  and  $Q_4$ .

Similar to  $K$  (Fig. 8), the mirror nature of the effect of  $Q_2$  and  $Q_4$  on  $\delta$ -ferrite  $P_\delta$  is manifested.

Fig. 11 shows the correlation between  $K$  and the total content of the combined elements  $Q_6=S+P+N+C+Si+Mn$  and  $Q_8=S+P+N+C+Si+Mn+Ni+Cr$ .

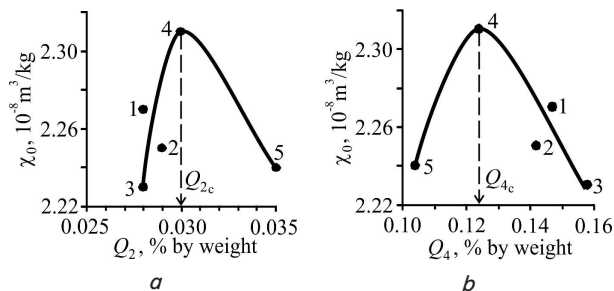


Fig. 9. Correlation between austenite's  $\chi_0$  and the total content of combined chemical elements:  $a - Q_2$ ;  $b - Q_4$

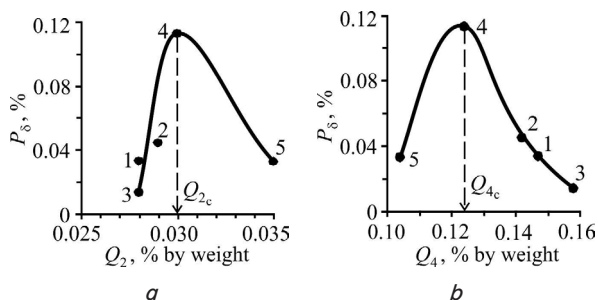


Fig. 10. Correlation between  $\delta$ -ferrite  $P_\delta$  and the total content of combined chemical elements:  $a - Q_2$ ;  $b - Q_4$

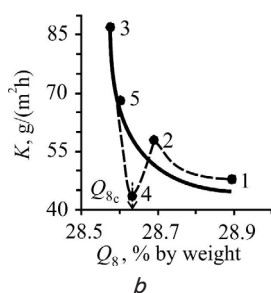
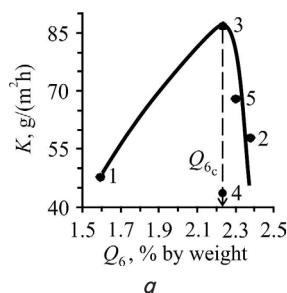


Fig. 11. Correlation between the rate of pitting corrosion  $K$  and the total content of combined chemical elements:  $a - Q_6$ ;  $b - Q_8$

The rate of corrosion  $K$  in the interval to the critical value of the elements (smelting 3)  $Q_6$  increases (smelting 1→smelting 3), and then decreases – (smelting 3→smelting 5→smelting 2→smelting 4).

The dependence of  $K$  on the estimated sum of all eight elements  $Q_8=S+P+N+C+Si+Mn+Ni+Cr$  coincides with the sum of the same elements ( $Q_8=Q$ ) of steel melting samples that were subjected to experimental measurements of  $K$ ,  $\chi_0$  and  $P_\delta$ .  $K$ 's dependence on  $Q_8$  is almost hyperbolic in nature, and the more precise dependence is shown by the dotted line in Fig. 11,  $b$ .

Fig. 12 shows the correlation between  $\chi_0$  and the total content of the combined elements  $Q_6$  and  $Q_8$ .

Comparing the estimated curves in Fig. 12 with experimental curves in Fig. 3, we have a proof of the correlation between  $K$  and the elements  $Q_6$  and  $Q_8$ .

Fig. 13 demonstrates the correlation between  $\delta$ -ferrite  $P_\delta$  and the total content of the combined chemical elements  $Q_6$  and  $Q_8$ .

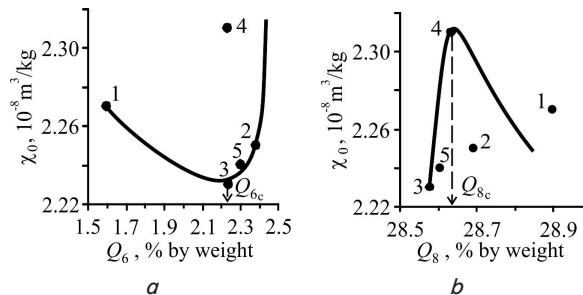


Fig. 12. Correlation between austenite's  $\chi_0$  and the total content of combined chemical elements:  $a - Q_6$ ;  $b - Q_8$

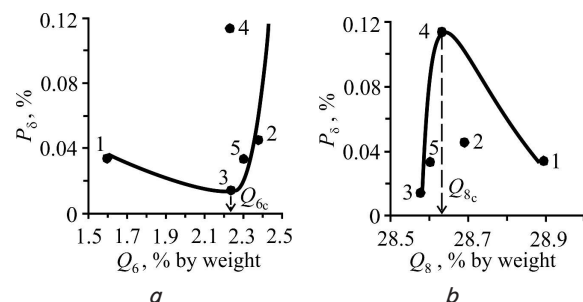


Fig. 13. Correlation between  $\delta$ -ferrite  $P_\delta$  and the total content of combined chemical elements:  $a - Q_6$ ;  $b - Q_8$

Comparing the calculated curves in Fig. 13 with experimental curves in Fig. 4, we have a proof of the correlation between the speed  $K$  and the content of the elements  $Q_6$  and  $Q_8$ .

## 6. Discussion of results of studying the role of individual and combined chemical elements (in the presence of others) on $K$ , $\chi_0$ , $P_\delta$

Most experimental methods (mass, radiometric, X-ray spectral, electrochemical, etc.) determine a parameter that is not integrated. That is, the measuring value does not characterize the substance as a whole but reflects only part of the properties (for example, the lattice parameter determines the geometry of the crystal, registering the boundaries indicates the presence of phases, etc.). The integrated parameter makes it possible to display all the components of the formed austenite's matrix not only by the presence of chemical elements but also due to mechanical and temperature effects.

This parameter can be a specific magnetic susceptibility  $\chi_0$  of austenite. This parameter characterizes the atomic magnetic state of the austenite matrix and is sensitive to external factors. It is necessary not to confuse the specific magnetic susceptibility  $\chi_0$  of austenite ( $\gamma$ -phase) with the magnetic susceptibility of the sample  $\chi$ , which is essentially two-phase ( $\gamma+\delta$ ) [28]. Along with  $\chi_0$ , it is possible to use in parallel, as a parameter, a low content of  $\delta$ -ferrite  $P_\delta$ , if it is present. To answer the questions posed, it is assumed that a significant parameter with which corrosion speed correlates is the paramagnetic susceptibility of austenite. Because its content is more than 95% and it has the largest touch surface with an aggressive environment, austenite is characterized by a specific magnetic susceptibility  $\chi_0$ , which is numerically equal to the sum of spin and orbital moments of a unit of mass at a single value of the magnetic field. Thus, such a

different rate of pitting corrosion in different smelting cycles is explained by a change in the magnetic state of austenite due to a different combination of chemical elements.

However, regardless of the order of location of the elements, the sum of their percentage contents in each model remains unchanged, that is, equal to the sum  $Q$  of all alloying elements contained in the samples from all smelting cycles ( $Q=Q_8$ ). At the same time, this is based on the fact that  $\chi_0$  and  $P_\delta$  have been experimentally determined for these samples.

On the parabolic curves of dependences  $K$ , the specific magnetic susceptibility  $\chi_0$  and  $P_\delta$  on the concentration of elements established the points (min or max) of critical contents of individual and combined elements, before and after which the rate of pitting corrosion decreases or increases.

Comparing the curves of the presented models in Fig. 1–13 with experimental curves  $K(\chi_0)$  and  $K(P_\delta)$  (Fig. 3), one can track the role of individual and combined elements on the change in the corrosion rate  $K$  in smelting cycles 1–5.

For individual elements P and C in intervals up to their critical content, the speed  $K$  decreases ( $\chi_0$ ,  $P_\delta$  increase), and after –  $K$  increases ( $\chi_0$ ,  $P_\delta$  decrease) (Fig. 1–3). And for the components Mn and Cr, vice versa (Fig. 5–7). For individual elements P and C, the rate of pitting corrosion is opposite in the intervals before and after critical contents. In this case, P and C can play both positive and negative roles, that is, there is an extremum in the dependences  $K(P)$  and  $K(C)$  (Fig. 1).

The components Mn and Cr act on a corrosive speed in the same direction in the intervals before and after critical contents and play both a positive and negative role (Fig. 5).

Using the example of combined elements  $Q_2=S+P$  (Fig. 8, *a*),  $Q_4=S+P+N+C$  (Fig. 8, *b*),  $Q_6=S+P+N+C+Si+Mn$  (Fig. 11, *a*),  $Q_8=S+P+N+C+Si+Mn+Ni+Cr$  (Fig. 11, *b*), we observe a more complex process of corrosion due to the action of two or more elements at the same time. One direction of action of the combined elements (Fig. 8, 11) is not noticed at a corrosion rate in intervals before and after critical contents. A decrease in the corrosion rate  $K$  was detected depending on  $Q_2$  (Fig. 11, *a*) to critical contents in smelting cycles 3, 2, 1, 4; on  $Q_4$  (Fig. 11, *b*) in smelting cycles 5, 4; on  $Q_8$  (Fig. 11, *b*) in smelting cycles 3, 5, 2, 1, 4; and, on  $Q_6$  (Fig. 11, *a*), there is an increase in  $K$ .

It should be noted that for other models (any permutation of elements) there will be other shapes of the above dependence curves (Fig. 8–13). However, for the sum of all elements, the shape of the curves remains the same for all models. In the presented models, an ambiguous (parabolic) role of components in the behavior of pitting corrosion was found (Fig. 1–13). Given this, it is assumed that one value of  $K$ ,  $\chi_0$ ,  $P_\delta$  can correspond to

several values (in intervals before and after critical content) of the percentage of the content of the elements.

A feature of the proposed method is the study of the effect of chemical elements on corrosion in different smelting cycles of the same steel grade. The limited nature of the study by the suggested method is that it is used only for paramagnetic austenitic steels (phase composition:  $\gamma$ -phase or  $\gamma+\delta$ , subject to the content of  $\delta$ -ferrite up to 1 %).

Summing up the discussion of the results obtained, it should be noted that such a positive and negative role can be explained by the total content of spin and orbital moments of the paramagnetic state of the austenite's matrix. The corresponding total magnetic moment is induced by the composition of chemical elements, the influence of temperature and deformation effects even before the tests for pitting corrosion. This also explains the ambiguous behavior of pitting resistance of individual and combined elements.

It should be noted that the proposed magnetometric method is suitable for determining and explaining changes in pitting corrosion not only for smelting cycles of the same grade but also for melting different grades of steel with a close content of elements. Thus, the AISI 321 steel mainly differs from the AISI 304 steel by a content of ~1 % more than Ni and a smaller content of Cr by ~1 %, as well as the presence of Ti within 0.3–0.4 % by weight. However, the corrosion rate in the five smelting cycles of each grade varied for AISI 321 in the range of 75–130 g/(m<sup>2</sup>h) [29], and in AISI 304 – 40–85 g/(m<sup>2</sup>h). Such a change in corrosion rate can be traced via the atomic magnetic state of austenite, that is, by a change in the specific magnetic susceptibility  $\chi_0$ .

## 7. Conclusions

1. It has been established, based on the example of individual P, C, Mn, Cr elements of the steel AISI 304 smelting cycles, that there is a correlation relationship between the rate of pitting corrosion and magnetic susceptibility of austenite, the content of  $\delta$ -ferrite, the percentage of elements. The ambiguous role of both individual and combined elements was determined.

2. The example of the combined elements  $Q_2=S+P$  and  $Q_4=S+P+N+C$  shows that the change in corrosion rate is, respectively, opposite in the intervals before and after their critical contents. For elements  $Q_6=S+P+N+C+Si+Mn$ , the corrosion rate increases in the interval to their critical content, and then decreases. For elements  $Q_8=S+P+N+C+Si+Mn+Ni+Cr$  of the steel AISI 304 smelting cycles, the corrosion rate decreases with increasing content of all elements.

## References

1. Khoma, M. C. (2021). State and prospects of research development in the field of corrosion and corrosion protection of construction materials in Ukraine: According to the materials of report at the meeting of the Presidium of NAS of Ukraine, October 27, 2021. *Visnyk of the National Academy of Sciences of Ukraine*, 12, 99–106. doi: <https://doi.org/10.15407/visn2021.12.099>
2. Biehler, J., Hoche, H., Oechsner, M. (2017). Corrosion properties of polished and shot-peened austenitic stainless steel 304L and 316L with and without plasma nitriding. *Surface and Coatings Technology*, 313, 40–46. doi: <https://doi.org/10.1016/j.surfcoat.2017.01.050>
3. Lochyński, P., Domańska, M., Kasprzyk, K. (2019). Corrosion of the chromium-nickel steel screenings and grit separator. *Ochrona przed Korozją*, 62 (7), 225–235. doi: <https://doi.org/10.15199/40.2019.7.2>
4. Shejko, S., Mishchenko, V., Tretiak, V., Shalomoev, V., Sukhomlin, G. (2018). Formation of the Grain Boundary Structure of Low-Alloyed Steels in the Process of Plastic Deformation. *Contributed Papers from MS&T17*. doi: [https://doi.org/10.7449/2018/mst\\_2018\\_746\\_753](https://doi.org/10.7449/2018/mst_2018_746_753)
5. Sabooni, S., Rashtchi, H., Eslami, A., Karimzadeh, F., Enayati, M. H., Raeissi, K. et. al. (2017). Dependence of corrosion properties of AISI 304L stainless steel on the austenite grain size. *International Journal of Materials Research*, 108 (7), 552–559. doi: <https://doi.org/10.3139/146.111512>

6. Ha, H.-Y., Jang, J., Lee, T.-H., Won, C., Lee, C.-H., Moon, J., Lee, C.-G. (2018). Investigation of the Localized Corrosion and Passive Behavior of Type 304 Stainless Steels with 0.2–1.8 wt % B. *Materials*, 11 (11), 2097. doi: <https://doi.org/10.3390/ma11112097>
7. Tolulope Loto, R. (2017). Study of the Corrosion Resistance of Type 304L and 316 Austenitic Stainless Steels in Acid Chloride Solution. *Oriental Journal of Chemistry*, 33 (3), 1090–1096. doi: <https://doi.org/10.13005/ojc/330304>
8. Wang, X., Yang, Z., Wang, Z., Shi, Q., Xu, B., Zhou, C., Zhang, L. (2019). The influence of copper on the stress corrosion cracking of 304 stainless steel. *Applied Surface Science*, 478, 492–498. doi: <https://doi.org/10.1016/j.apsusc.2019.01.291>
9. Loable, C., Viçosa, I. N., Mesquita, T. J., Mantel, M., Nogueira, R. P., Berthomé, G. et. al. (2017). Synergy between molybdenum and nitrogen on the pitting corrosion and passive film resistance of austenitic stainless steels as a pH-dependent effect. *Materials Chemistry and Physics*, 186, 237–245. doi: <https://doi.org/10.1016/j.matchemphys.2016.10.049>
10. Azhazha, V. M., Desnenko, V. A., Ozhigov, L. S., Azhazha, Zh. S., Svechikaryov, I. V., Fedorchenko, A. V. (2009). The use of magnetic methods for investigating the structure evolution in austenitic stainless steels after a long-term service at nuclear power plant units. *Voprosy atomnoy nauki i tekhniki. Ser.: Fizika radiatsionnykh povrezhdeniy i radiatsionnoe materialovedenie*, 94, 241–246. Available at: <http://dspace.nbu.gov.ua/bitstream/handle/123456789/96382/31-Azhazha.pdf?sequence=1>
11. Snizhnoi, G., Snizhnoi, V. (2020). Magnetometric method for investigation the effect of carbon and nitrogen on the corrosion resistance of austenitic chromium-nickel steels. *Aerospace technic and technology*, 7 (167), 47–51. doi: <https://doi.org/10.32620/akt.2020.7.07>
12. Narivsky, O., Belikov, S. (2018). Modern ideas about pitting corrosion of corrosion-resistant steels and alloys. *New Materials and Technologies in Metallurgy and Mechanical Engineering*, 2, 14–24. doi: <https://doi.org/10.15588/1607-6885-2018-2-2>
13. Narivskiy, A. (2013). Laws and mechanisms of corrosion dissolution of steel AISI 304 when working model sediment in waters. *Novi materialy i tekhnolohiyi v metalurhiyi ta mashynobuduvanni*, 1, 39–50. Available at: [http://nbuv.gov.ua/UJRN/Nmt\\_2013\\_1\\_11](http://nbuv.gov.ua/UJRN/Nmt_2013_1_11)
14. Narivskiy, A. E., Yar-Mukhamedova, G. Sh. (2016). Influence alloying elements and steel AISI 321 structural heterogeneity on the selective dissolution of metals from pitting. *Vesnik KazNU. Seriya fizicheskaya*, 56 (1), 86–96. Available at: <https://bph.kaznu.kz/index.php/zhuzhu/article/view/444>
15. Belikov, S. B., Narivskiy, O. E., Khoma, M. S. (2019). Pitinhova koroziya teploobminnykh v oborotnykh vodakh ta yii prohnouzuvannia. *Zaporizhzhia: NU «Zaporizka politekhnika»*, 216. Available at: <http://eir.zntu.edu.ua/handle/123456789/5053>
16. Belykov, S., Narivskiy, A. (2011). Kinetics of steel AISI 321 and 12X18H10T corrosion process in neutral chloride-containing solutions and corrosion rate. *Novi materialy ta tekhnolohiyi v metalurhiyi ta mashynobuduvanni*, 1, 36–44. Available at: <http://nmt.zntu.edu.ua/article/view/98965/94129>
17. Narivskiy, O. E., Solidor, N. A. (2011). Corrosion processes and growth rate of AISI 304 and 08X18H10T steel pitting in model circulating waters. *Visnyk Pryazovskoho derzhavnogo tekhnichnoho universytetu*, 2 (23), 87–97. Available at: [http://nbuv.gov.ua/UJRN/vpdy\\_2011\\_23\\_14](http://nbuv.gov.ua/UJRN/vpdy_2011_23_14)
18. Wang, J., Zhang, L. F. (2017). Effects of cold deformation on electrochemical corrosion behaviors of 304 stainless steel. *Anti-Corrosion Methods and Materials*, 64 (2), 252–262. doi: <https://doi.org/10.1108/acmm-12-2015-1620>
19. Pisarevskii, L. A., Filippov, G. A., Lipatov, A. A. (2016). Effect of N, Mo, and Si on Local Corrosion Resistance of Unstabilized Cr–Ni and Cr–Mn–Ni Austenitic Steels. *Metallurgist*, 60 (7-8), 822–831. doi: <https://doi.org/10.1007/s11015-016-0372-x>
20. Lutton Cwalina, K., Demarest, C. R., Gerard, A. Y., Scully, J. R. (2019). Revisiting the effects of molybdenum and tungsten alloying on corrosion behavior of nickel-chromium alloys in aqueous corrosion. *Current Opinion in Solid State and Materials Science*, 23 (3), 129–141. doi: <https://doi.org/10.1016/j.cossms.2019.03.002>
21. Osoba, L. O., Elemuren, R. A., Ekpe, I. C. (2016). Influence of delta ferrite on corrosion susceptibility of AISI 304 austenitic stainless steel. *Cogent Engineering*, 3 (1), 1150546. doi: <https://doi.org/10.1080/23311916.2016.1150546>
22. Ha, H.-Y., Lee, T.-H., Bae, J.-H., Chun, D. (2018). Molybdenum Effects on Pitting Corrosion Resistance of FeCrMnMoNC Austenitic Stainless Steels. *Metals*, 8 (8), 653. doi: <https://doi.org/10.3390/met8080653>
23. Lu, C., Yi, H., Liu, K. (2021). Effect of Si and Mn on microstructure and tensile properties of austenitic stainless steel. *Rare metal materials and engineering*, 50 (1), 187–194. Available at: [http://ir.imr.ac.cn/handle/321006/161036?mode=full&submit\\_simple>Show+full+item+record](http://ir.imr.ac.cn/handle/321006/161036?mode=full&submit_simple>Show+full+item+record)
24. Karki, V., Singh, M. (2017). Investigation of corrosion mechanism in Type 304 stainless steel under different corrosive environments: A SIMS study. *International Journal of Mass Spectrometry*, 421, 51–60. doi: <https://doi.org/10.1016/j.ijms.2017.06.001>
25. Snezhnoy, G. V., Mischenko, V. G., Snezhnoy, V. L. (2009). Integral'nyy fizicheskiy metod identifikatsii a-fazy v austenitnykh khromonikelevykh stalyakh. *Lit'e i metallurgiya*, 3 (52), 241–244. Available at: [https://scholar.google.com.ua/citations?view\\_op=view\\_citation&hl=ru&user=PmqVjMoAAAAJ&citation\\_for\\_view=PmqVjMoAAAAJ:2P1L\\_qKh6hAC](https://scholar.google.com.ua/citations?view_op=view_citation&hl=ru&user=PmqVjMoAAAAJ&citation_for_view=PmqVjMoAAAAJ:2P1L_qKh6hAC)
26. Mishchenko, V. G., Snizhnoi, G. V., Narivskiy, O. Eh. (2011) Magnetometric investigations of corrosion behaviour of AISI 304 steel in chloride-containing environment. *Metallofizika i Noveishie Tekhnologii*, 33 (6), 769–774. Available at: <https://mfint.imp.kiev.ua/en/toc/v33/i06.html>
27. Snizhnoi, G. V. (2013). Dependence of the Corrosion Behavior of Austenitic Chromium-Nickel Steels on the Paramagnetic State of Austenite. *Materials Science*, 49 (3), 341–346. doi: <https://doi.org/10.1007/s11003-013-9620-4>
28. Ol'shanetskiy, V. E., Snezhnoy, G. V., Snezhnoy, V. L. (2018). Special Features of Formation of Martensitic Phases in the Austenite of Chromium-Nickel Steels under Plastic Deformation. *Metal Science and Heat Treatment*, 60 (3-4), 165–171. doi: <https://doi.org/10.1007/s11041-018-0255-9>
29. Snizhnoi, G., Snizhnoi, V. (2021). Quality control of chrome-nickel steels by the paramagnetic state of austenite. *Aerospace technic and technology*, 3 (171), 79–83. doi: <https://doi.org/10.32620/akt.2021.3.09>